Limiting Light Escape Angle in Silicon Photovoltaics: Ideal and Realistic Cells

Emily D. Kosten, Bonna K. Newman, *Member, IEEE*, John V. Lloyd, Albert Polman, and Harry A. Atwater, *Member, IEEE*

ABSTRACT

Restricting the external light escape angle within a solar cell significantly enhances light trapping, resulting in potentially higher efficiency in thinner cells. Using an improved detailed balance model for silicon, we calculate the maximum efficiency gain of $3\%_{\text{abs}}$ efficiency gain for an ideal Si cell of 3 μm thickness and the escape angle restricted to 2.767° under AM1.5 direct illumination. Applying the model to current high-efficiency cell technologies, we find that a heterojunction type device, with better surface and contact passivation but more parasitic absorption losses, is better suited to escape angle restriction than a homojunction type device. In these more realistic cell models, we also find that there is little benefit gained by restricting the escape angle to less than 10°. The benefits of combining moderate escape angle restriction with low to moderate concentration offers further efficiency gains. Finally, we consider two potential structures for escape angle restriction: a narrowband graded index optical multilayer and a broadband ray optical structure. The broadband structure, which provides greater angle restriction, allows for higher efficiencies and much thinner cells than the narrowband structure.

***Index Terms*—Si solar cells, escape angle restriction, high efficiency**

I. INTRODUCTION

Silicon solar cells are currently the dominant terrestrial photovoltaic technology due to material abundance and relatively low-cost manufacturing processes and conversion efficiency continues to improve. Recently a new performance record of 25.6% was achieved [1]. One approach to increasing efficiency is restricting the angles at which light may escape the cells with an external optic. Restricting the escape angle reduces the escape cone inside the cell leading to two potential improvements: enhanced light trapping and increased photon recycling [2]–[4]. In materials with significant radiative recombination such as GaAs, the photon recycling effect is significant [5]–[7]. However, in low radiative efficiency materials, like silicon, the light trapping effect is more dominant, as light near the band edge is more completely absorbed [2], [3]. Limiting the light escape angle significantly enhances the light trapping mechanisms already utilized in current flat-plate silicon cells, allowing for excellent light absorption in a very thin cell and reduced materials usage.

While the limiting efficiencies for silicon cells under angle restriction were initially calculated by Campbell and Green in 1986 [3], we re-calculate these efficiencies to include models for free carrier absorption [8], improved Auger parameterizations [9], and bandgap narrowing [10] that have been developed in the intervening decades. Using this model we calculated a gain of $3\%_{\text{abs}}$ efficiency increase for an Auger-limited cell with maximum angle restriction (2.767°) and considering only the direct portion of the spectrum. We further develop the model to include surface and Shockley-Reed-Hall (SRH) recombination, allowing us to simulate the performance of current heterojunction and homojunction technologies [11]–[13]. We find that heterojuntion cells should be more ideal for angle restriction due to the lower surface recombination and the potential for thinner cells. We also find that excellent surface recombination and back reflectivity are crucial for significant efficiency improvements with angle restriction, as we would expect with thinner cells, while bulk lifetime has less impact.

When the escape angle is limited, the angles at which light can enter the cell are also limited, as a consequence of optical reciprocity. Thereby, escape angle restriction will also limit the portion of the diffuse spectrum that can be used by the device and the practical impact of escape angle restriction will depend upon the amount of diffuse light in a given location. However, for a concentrator system, the light is limited mostly to the direct portion of the spectrum as well. In these cases, we find that the gains from escape angle restriction are more clear and that combining moderate angler restriction with moderate concentration can offer potentially more flexibility in system design and higher efficiencies.

There has been significant previous work on various designs for achieving angle restriction in silicon cells [3], [14]–[17].

Manuscript received June XX, 2014. E.K. and H.A. are supported by the Light-Matter Interactions Energy Frontier Research Center, an EFRC program of the Office of Science, United States Department of Energy under grant DE-SC0001293. E.K. is also the recipient of a Resnick Sustainability Institute Graduate Fellowship. J.L. is supported by funding from the DOW Chemical Company. Work at the Center for Nanophotonics at AMOLF is part of the research program of FOM which is financially supported by NWO. It is also supported by the European Research Council.

E. D. Kosten and B. K. Newman contributed equally to this work.

E. D. Kosten, J. V. Lloyd, and H. A. Atwater are with the Thomas J. Watson Laboratory of Applied Physics, California Institute of Technology, Pasadena, CA 91125, USA (e-mail:haa@caltech.edu)

B. K. Newman was with the Center for Nanophotonics, FOM Institute AMOLF, 1098 XG Amsterdam, The Netherlands. She is now with ECN Solar Energy, 1755 ZG Petten, The Netherlands.

A. Polman is with the Center for Nanophotonics, FOM Institute AMOLF, 1098 XG Amsterdam, The Netherlands.

Color versions of one or more of the figures in this paper are available online at http://ieeexplore.ieee.org.

Digital Object Identifier 10.1109/

However, most of these have focused on increasing short circuit currents in very thin idealized cells. In contrast, we explore the effects of both narrowband rugate structures and broadband ray optical structures for angle restriction, over a wide range of cell thicknesses and for both ideal and realistic cells. We find that broadband ray optical angle restrictors allow for much larger efficiency enhancements than their narrowband counterparts, owing to the narrower angle restriction provided over a broader range of wavelengths. With a broadband structure, efficiency increases up to 0.8%$_{\text{abs}}$ for heterojunction type cells and 1.5%$_{\text{abs}}$ for idealized cells are predicted for optimal cell thicknesses.

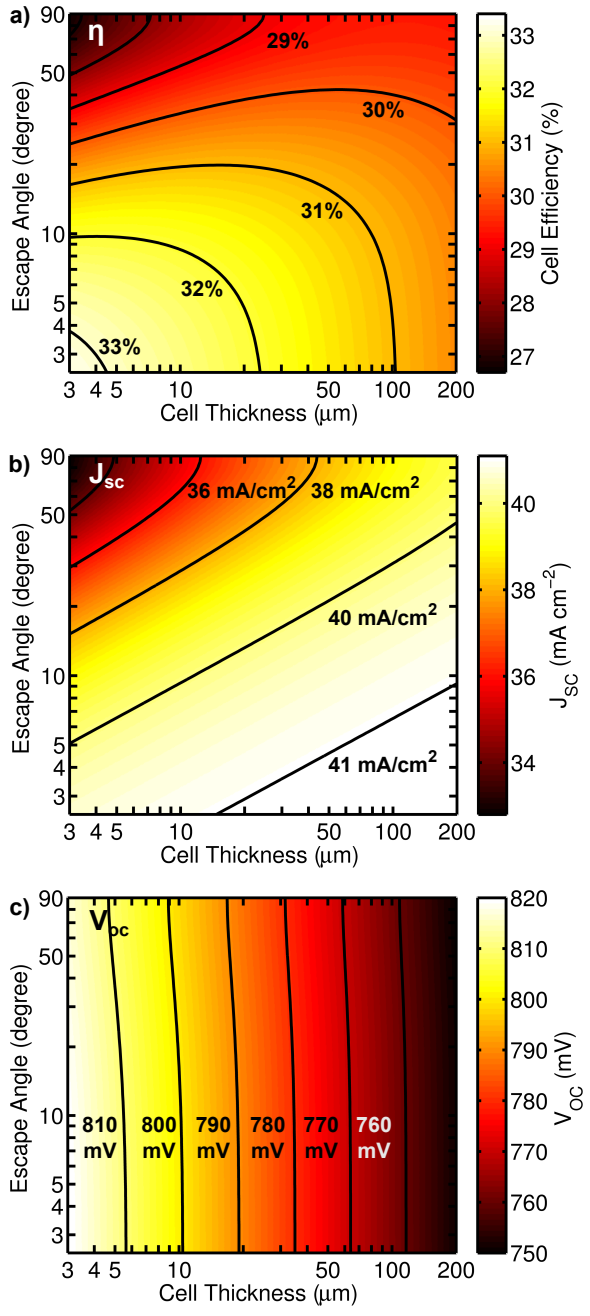

Fig. 1. Efficiency η, short circuit current, J_{SC}, and open circuit voltage, V_{OC}, for an ideal, Auger-limited silicon solar cell as a function of cell thickness and emission angle, under AM1.5 direct spectrum illumination. Efficiency is reported with respect to 90 mW cm^{-2} power flux. Increases in both J_{SC} and V_{OC} are observed by limiting escape angle and cell thickness respectively. Narrow angle restriction and a very thin cell lead to the highest efficiency.

II. Effects of Angle Restriction in Ideal and Realistic Silicon Cells

To model the effects of angle restriction we use a detailed balance approach, assuming intrinsic silicon, with uniform carrier density throughout the absorber layer, and excellent carrier collection [18]. The net current, $J(V)$, is given by

$$J(V) = J_L(V) - R_A(n,p,n_0,p_0)W - R_{RR} - J_{SRH} - J_{SRV}. \quad (1)$$

Here, $J_L(V)$ is the light generated current is given by:

$$J_L(V) = C_f \int_0^\infty a(E,V)S(E)dE.$$

Where S(E) is the AM 1.5 direct solar spectrum and C_f is the external concentration factor, with voltage dependence owing to the free carrier absorption. The band-to-band absorptivity, $a(E)$, is:

$$a(E) = \frac{\alpha(E)}{\alpha(E) + \alpha'(E) + \frac{\sin^2(\theta_e)}{4n_r^2 W}} \quad (2)$$

where $\alpha(E)$ and $\alpha'(E)$ are the band to band and parasitic absorption coefficients respectively, and θ_e is the angle defining the escape cone. [2], [3], [19]. Thus, as the escape angle, θ_e, is reduced, $a(E)$ increases, as the escape cone for light within the solar cell narrows.

In second term of (1), the quantity $R_A(n,p,n_0,p_0)$ is Auger recombination as a function of the electron and hole concentrations based on the recent parameterization determined by Richter et. al. [8], [9], [18]. As Auger recombination is a bulk process, this term scales with the cell thickness, W. Electron and hole concentrations are determined from the assumed doping, the neutrality condition, the cell voltage, and the law of mass action [20]. Band gap narrowing is also included this term with intrinsic carrier concentration, $n_{i,0}$ of 8.28x10^9 cm^{-3} [8], [10], [21], [22] at T = 25°C.

The third term in (1), R_{RR}, accounts for current losses due to radiative recombination processes. This is modeled as blackbody type radiative emission at each photon energy E and applied voltage V, and allows us to include angle restriction as follows:

$$R_{RR} = \int_0^\infty \frac{2}{h^3c^2}\frac{E^2}{e^{(E-qV)/kT}-1} \times \left(\int_{\Omega_c} a(E)cos(\theta)d\Omega + \pi n_r^2 a'(E)\right)dE. \quad (3)$$

Where h is Planck's constant, c is the speed of light, q is electron charge, and k is Boltzmann's constant. The first term accounts for the radiative emission from the material with absorptivity, $a(E)$, in the solid angle Ω_c. For a planar emission with escape angle restriction this term integrates to $\sin^2(\theta_e)$.

The second term is the parasitic absorptivity of spontaneously emitted light, $a'(E)$, weighted by the square of the silicon refractive index, n_r, to account for the relative concentration of light within the solar cell [4], [18], [19], [23], [24]. The parasitic absorptivity is given by:

$$a'(E) = 4W\alpha'(E)\frac{\alpha(E)}{\alpha(E)+\alpha'(E)+\frac{\sin^2(\theta_e)}{4n_r^2W}} \quad (4)$$

where the amount of parasitic absorption is proportional to both the band-to-band emission, and the parasitic absorption coefficient, $\alpha'(E)$ [4], [23], [25]. Absorption in non-ideal back reflectors is included along with free carrier absorption in the parasitic absorption coefficient:

$$\alpha'(E) = \alpha_{FCA} + \frac{1-R_b}{4W} \quad (5)$$

where $\alpha_{FCA}(E)$ is the free carrier absorption coefficient and R_b is the back reflectivity [25].

Finally, for more realistic cell models, we also include other types of non-radiative recombination,

$$J_{SRH} = \frac{qW}{\tau_B}\frac{np-n_{ieff}^2}{p+n}$$

$$J_{SRV} = 2qS\frac{np-n_{ieff}^2}{p+n}$$

where τ_B is the bulk lifetime associated with SRH processes, and S is the surface recombination velocity (SRV) [26]. For both of these expressions, we assume a single SRV and SRH lifetime averaged over both carrier types, and, in the case of the SRV, both surfaces.

Using these relations, we calculate the maximum power under angle restriction as well as short circuit current, J_{SC}, and open circuit voltage, V_{OC}. Because the amount and angular distribution of diffuse light will vary significantly depending on location, we calculate the cell performance respect to only the AM1.5 direct spectrum [27] and efficiency is normalized to 90 W cm^{-2} irradiance. We will discuss the potential impact of diffuse light below.

A. Angle Restriction in Ideal Cells

Figure 1 shows the results for an n-type, lowly-doped (1x10^{11} cm^{-3}) silicon substrate assuming a perfect back reflector and neglecting all non-radiative recombination other than Auger. Highest efficiency, up to a 3%$_{\text{abs}}$ increase, is achieved for thinner cells with narrow angle restriction. While thinner cells show improved performance, we limit the minimum cell thickness to 3 μm, as the absorptivity expressions above apply only in the ray optical limit. Additionally, thinner cells are not optimal when more realistic losses are considered, as described in the next section. Most of the enhancement at a given thickness is due to improved light trapping and a corresponding increase in J_{SC} (Figure 1b) with less effect from photon recycling impacting V_{OC} (Figure 1c). The V_{OC} is mostly improved by thinning the cell, as losses from Auger recombination are reduced.

From the efficiency, Figure 1a, we can discern the optimum thickness at a given angle restriction. With no angle restriction (θ_e = 90°), under AM1.5 direct illumination, we find the maximum ideal solar cell efficiency of 29.4% with the optimal thickness of approximately 118 μm (in good agreement with previous calculations under AM1.5 global illumination [9]). As the angle restriction narrows, the optimal thickness decreases as well. While narrow angle restriction and very thin cells lead to the highest efficiencies, for cells thicker than about 50 μm, angle restriction narrower than 10° has less impact on cell performance, suggesting that improvement for wafer-based silicon cells may be achievable even with less restrictive escape angles.

B. Angle Restriction in Realistic Cells

While the limiting efficiency case is of theoretical interest, it is also important to consider the effects of angle restriction on current production-type silicon solar cell technologies: a-Si/c-Si heterojunctions with lower surface and contact recombination and homojunction devices. For this reason, we include additional losses due to bulk SRH and surface recombination in (1) as well as including imperfect back reflectors to account for parasitic losses within the cell.

Table 1 summarizes the parameters used in all three cell models: ideal, homojunction and heterojunction. Back surface reflectance, cell thickness, and thickness of the a-Si for the heterojunction cell are estimated for both cell types from published values where possible [11], [28]. With these estimates, effective surface recombination velocity and bulk Shockley-Read-Hall lifetimes are determined by fitting reported V_{OC} values for record or near-record cells under the AM 1.5 global spectrum [11]–[13]. Modelled efficiencies, V_{OC}, and optimal thickness for these reference cells with no angle restriction can be found in the bottom half of Table 1.

In Figure 2, there is a contrast in the effects of angle restriction in heterojunctions versus homojunctions, despite similar reported efficiencies for these two cells [13]. To see this more clearly, we consider the J_{SC} and V_{OC} values plotted in Figure 2. The absolute value of maximum J_{SC} under angle restriction is larger for the homojunction type device due to the lower parasitic losses for thick cells, but the relative gain in J_{SC} is greater in the heterojunction. The potential impact in V_{OC} is also greater in heterojunctions due to thinner cells and less impact from suface/contact recombination. For both cell types, at all thicknesses, most of the increase in efficiency occurs between 10°and 70°, suggesting that maximum angle restriction may not be necessary or optimal.

TABLE I
CELL PARAMETERS FOR IDEAL AND REALISTIC CELL MODELS.

	Ideal	heterojunction	homojunction
Dopant Density (cm^{-3})	1x10^{11}	1.6x10^{15}	1.6x10^{15}
Back Reflectivity (%)	100	98	95
SRV (cm s^{-1})	0	2.87	11.64
τ_B (ms)	Infinite	2.2	1.2
Reference Cells under Global Illumination and no Angle Restriction			
Eff.(%)	29.5	24.7	24.4
V_{oc} (mV)	762	750	721
Thickness (μm)	105	100	180

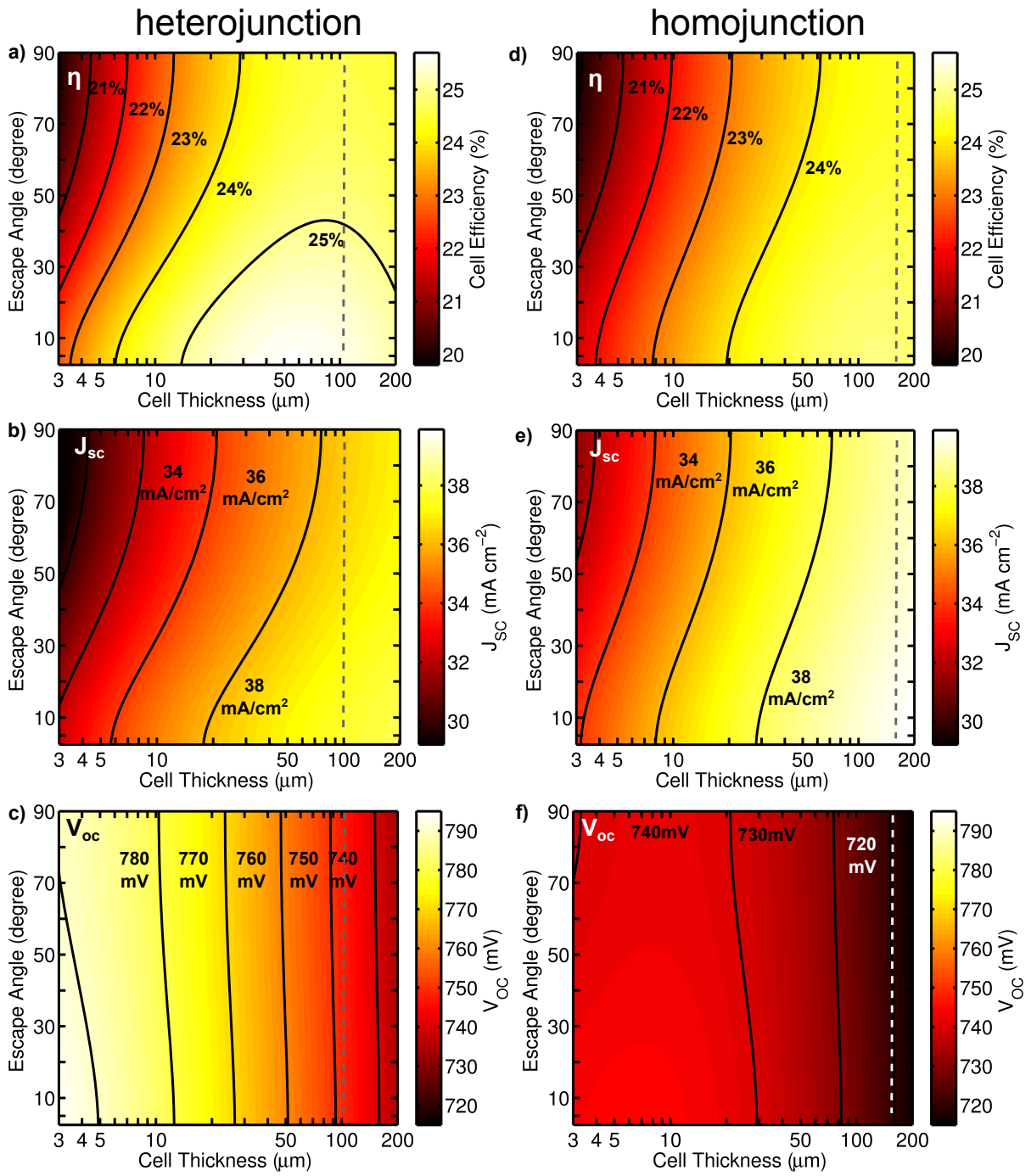

Fig. 2. Efficiency, η, short circuit current, J_{SC}, and open circuit voltage, V_{OC}, as a function of cell thickness and escape angle for cells with surface recombination and SRH lifetimes mimicking heterojunction and homojunction type silicon cells. Vertical dashed lines represent the thickness of the reference cells. Heterojunction cells show greater efficiency improvements with angle restriction.

Now we use the complete model to further explore the relative impact surface/contact recombination, bulk recombination, and back reflectivity in realistic cells. In Figures 3a and 3b we plot the efficiency and efficiency increase under angle restriction as a function of back reflectivity, and also examine the effect of a factor of two improvement in either SRV or bulk lifetime. While improvements in either back reflectivity, SRV, or lifetime lead to an overall efficiency enhancement, as shown in Figure 3a, SRV and back reflectivity lead to greater efficiency increase with angle restriction as shown in Figure 3b. As shown in Figure 3c, which gives the optimal cell thickness at 10°ângle restriction as a function of back reflectivity, improved SRV and back reflectivity lead to larger improvements with angle restriction as they allow for thinner optimal cells. In contrast, the optimal cell thickness under angle restriction is larger for longer lifetimes, as bulk

recombination is reduced. Thus, improving SRV and back reflectivity are crucial to achieving thin, high efficiency silicon cells under angle restriction.

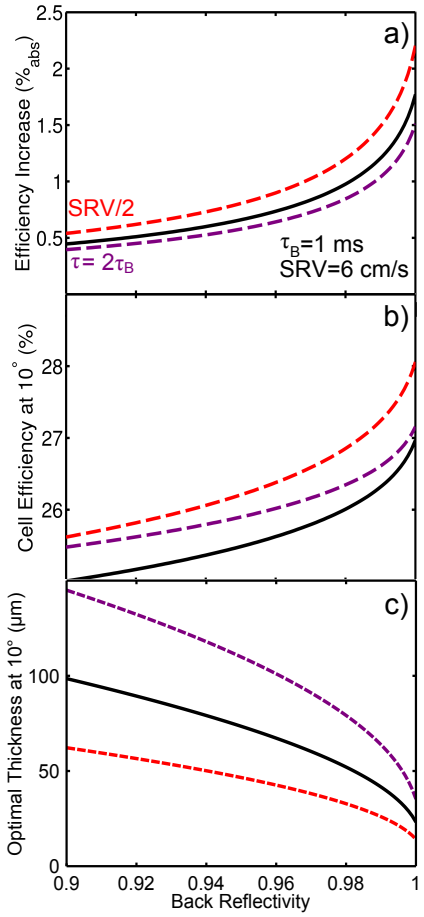

Fig. 3. Cell efficiency (a), efficiency increase (b), and optimal thickness (c) at 10°restricted angle, as a function of back reflectivity for a heterojunction-type cell with SRH lifetime τ_B = 1 ms and SRV = 6 cm s^{-1} (black), and the same data for τ_B = 2 ms (dashed purple), and SRV = 3 cm s^{-1} (dashed red).

C. Angle Restriction with External Concentration

So far, we have considered the effect of escape angle restriction for enhanced light trapping in the solar cell. Next we consider how external concentration can further enhance the performance of a Si device when used in combination with the same angle restriction geometry. An external concentrator will also limit the optical acceptance angle: light is collected from a limited range of incoming angles and concentrated onto a smaller area with a broader angular spread. At the thermodynamic limit [29] of concentration by the factor C_f, the relationship between the angular spread of incoming light, θ_{in}, and the angular spread of light after concentration, θ_{out} is

$$\sin(\theta_{out}) = \sqrt{C_f}\sin(\theta_{in}). \quad (6)$$

For solar radiation with perfect tracking, the direct spectrum is incident from a limited set of angles spanned by the image of the sun on the earth's surface and the spread of the circumsolar radiation [27]. Due to reciprocity, the angular spread of light after concentration limits the narrowest possible solar cell escape angle where all incoming light is collected.

In Figures 4a and 4b, we plot the efficiency and optimal thickness respectively of a heterojunction cell with angle restriction combined with various levels of concentration, neglecting heating or increased series resistance losses in the cells. Without concentration, efficiency can be improved up to 0.8%$_{abs}$ by narrowing the escape angle to 20°consistent with Figure 4a. With concentration, the optimal thickness increases due to the increased carrier density and increased recombination rates. Conversely, and similar to the case with no concentration, we see that the optimal thickness decreases with increased angle restriction (assuming no heating). Thus for a given concentration, higher efficiency could be reached with a thinner device.

As mentioned previously, an angle restriction scheme would likely require tracking to ensure the sun's image falls within the allowed angles for light to enter the cell. A typical low-precision tracking system for solar is on the order of 5°; performance limitations for such a tracker are also indicated in Figure 4. With such a tracking system, using 50x concentration in combination with moderate angle restriction of 40°, a heterojunction device could achieve greater than 30% efficiency (with respect to the direct spectrum) with a 100 μm substrate. The tradeoff between thickness, concentration, and angle restriction offers a variety of options for attaining higher efficiency with a range of various module geometries.

D. Impact of Diffuse Light

By reciprocity, any amount of angle restriction requires that we not use some fraction the diffuse part of the spectrum, which is at minimum 10% of the ambient light (in the case of the ASTM173 standards used here) and is often more significant depending on location. While there is little data on the angular distribution of the diffuse light, we suspect it is not globally distributed in high DNI locations, and that it is likely highly location dependent. Thus, we have restricted the calculations to only considering the direct portion of the spectrum, even for cells with no angle restriction. As a basic comparison, we examine the two endpoints: power output at maximum angle restriction (2.767°) and AM1.5 direct illumination compared to power output of the same cell with no angle restriction under global illumination. In the case of the ideal cell, we find a gain of 3.3 W m^{-2}. However, for the heterojunction and homojunction devices, we find a loss of 15.7 W m^{-2} and 21.4 W m^{-2} respectively. While this may not seem promising, moderate angle restriction seems likely to include a large portion of the diffuse light for many locations and could result in better average power output, even in realistic cells, and perhaps particularly when used in conjunction with external concentration. Thus, further location-specific data on the angular distribution of diffuse light is required to more accurately analyze the effectiveness of this approach from a power production standpoint, and determine the optimal degree of angle restriction and external concentration.

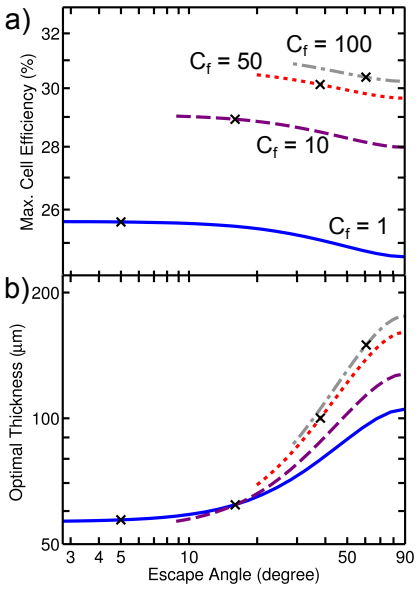

Fig. 4. Maximum cell efficiency (a) and corresponding optimal cell thickness (b) as a function of escape angle for an heterojunction-type cell with various external concentrations, C_f, assuming ideal tracking precision indicated by the lines. Results for 5°tracking precision are indicated by black 'x'.

III. Angle Restrictor Designs

In all the preceding calculations, we have assumed an ideal angle restrictor: lossless, with either 100% reflection or transmission, and no wavelength dependence. There has been significant prior work focused on designing such structures for both crystalline and amorphous silicon cells [3], [14]–[17]. However, most of this work has focused on structures that limit the escape angle only over a narrow wavelength range for very thin, idealized solar cells or has been more conceptual. Here, we consider both narrowband and broadband angle restrictors and analyze the effects of these structures on the performance of both the idealized and heterojunction silicon cells over a range of thicknesses.

A. Narrowband Angle Restrictor

To achieve narrowband angle restriction, we consider a multilayer structure with alternating high and low refractive index. While the design considered here is more sophisticated, the angle restriction effect may be understood by considering the Bragg condition for reflection from a periodic stack with alternating high and low index layers:

$$\cos\theta_m = \frac{m\lambda}{2\Gamma}$$

where θ_m is the angle of maximum reflectivity, λ is the wavelength, Γ is the period of the multilayer, and m is an integer [30]. Thus, for shorter wavelengths, maximum reflection occurs away from normal incidence, achieving the desired angle restriction effect. To avoid undesirable second-order reflecting bands, and other normal incidence reflections, we utilize a rugate structure, with a gradual variation of refractive index [15], [16], [31], [32]. We assume the cell is placed under glass (n=1.5), as is common in a module, and that gradual index variation between 1.5 and 2.5 may be achieved with SiO_2/TiO_2 co-deposition [33]–[35]. We also assume that the rugate structure is deposited in place of an anti-reflective (AR) coating between the glass and the solar cell. As a comparison case, we consider a graded index AR coating with a quintic-type refractive index profile deposited at the same interface and with the same range of refractive index [36]. The transfer-matrix method is used to calculate the performance of the thin film structures. Reflections off the overlying glass (n=1.5) were included with a multi-pass model. Figure 5a shows the refractive index profiles of the optimized rugate angle-restricting structure and the graded index coating.

The calculated reflectivity as a function of angle of incidence and wavelength for the two coatings is shown in Figures 5b and 5c. The reflectance at normal incidence is very similar for both cases. Thus, the rugate structure avoids additional optical losses. The rugate structure shows a sharp transition in reflectivity at a given angle, in the wavelength range 1050-1200 nm. In this wavelength range, the light escape cone is thus limited, as desired. As the angle restriction is relatively narrowband, the angle restrictor will capture diffuse incident light over most of the solar spectrum, which may also allow for simpler, cheaper tracking. However, this also means that cell will only have enhanced light trapping in the 1050 - 1200 nm range, limiting the potential impact for thin cells.

To calculate the performance of a cell with the rugate angle-restricting coating described above, we replace the factors of $\sin^2(\theta_e)$ in the model with a wavelength dependent angle-averaged transmission, determined from the reflectivity results shown in Figures 5b and 5c. As shown in Figure 5d, for an ideal cell, optimal thickness decreases from 110 μm to 80 μm. For the heterojunction cell, efficiency increases $0.3\%_{abs}$ with a 7 μm decrease in optimal thickness. The narrowband design also allows diffuse light to enter the cell over most of the solar spectrum. As discussed above, depending on the distribution of diffuse light, the rugate structure may offer more benefit not accounted for here.

B. Broadband Angle Restrictor

The results above suggest that narrower angle restriction over a broader wavelength range will be required to achieve the efficiency increases calculated for the ideal angle restrictor. To explore this further, we examined a broadband ray-optical angle restrictor, which utilizes an array of hexagonal solid compound parabolic concentrator (CPC) structures as shown in Figure 6a [29]. In this design, similar to that proposed by Green, the CPC structure utilizes total internal reflection to direct light near normal incidence to the output aperture where it enters the cell [3], [14]. Except for the area under the output apertures of the CPCs, the top surface of the cell is coated with a metallic reflector, such that light inside the cell can only escape through the output apertures and light trapping is enhanced.

As in the previous section, we assume that the CPC array and solar cell is under glass with index of 1.5. We also assume that the solid CPC structures have constant refractive index of 1.5, and that the graded-index AR coating presented in

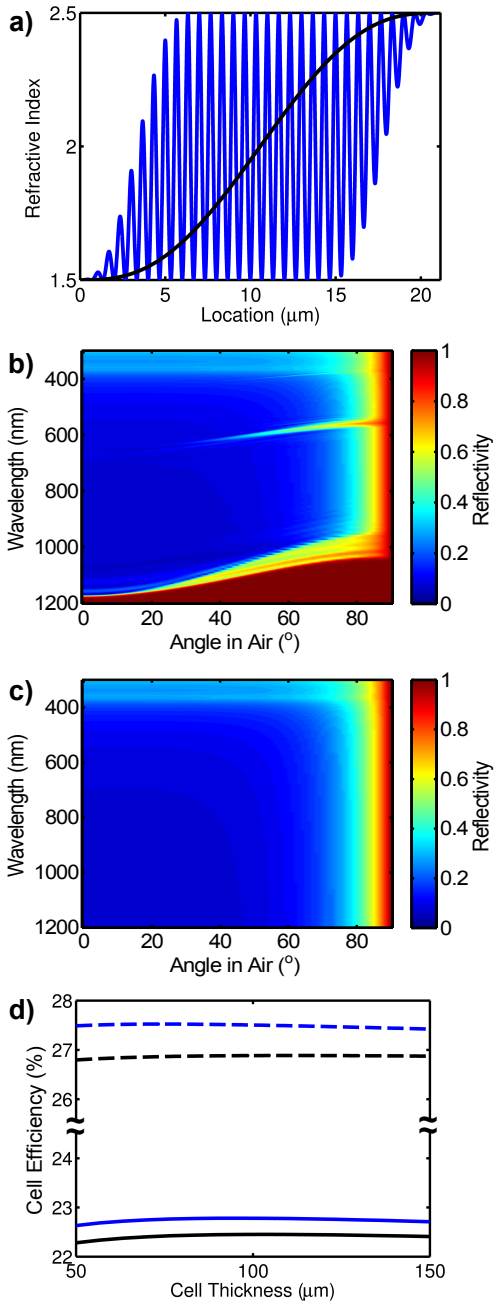

Fig. 5. a) Refractive index profile for rugate angle restrictor design (blue), and quintic graded index AR coating for comparison (black). b) Calculated reflectivity as a function of incident angle (relative to the surface normal) and wavelength, for rugate angle restrictor design and (c) graded index AR coating. d) Calculated efficiency as a function of cell thickness with rugate angle restrictor (blue) and graded index AR coating (black) for the heterojunction cell model (solid), and the ideal cell model (dashed).

Figure 5 is deposited between the CPC output apertures and the silicon cell below. Ray tracing simulations, were used to calculate the reflectivity as a function of incident angle for the wavelength range of interest, and representative results at 1000 nm are shown in Figure 6b. At other wavelengths, the reflectivity is similar with the small wavelength dependence due to the AR coating between the CPC array and the silicon below. We note that achieving narrow angle restriction with good transmission requires including a conical section at the bottom of the CPC to narrow the range of output angles from the structure and avoid rejected skew rays [29]. As shown in Figure 6b, the conical section leads to a higher aspect ratio structure. Ideally, however, the spacing between the reflector holes would be no larger than the carrier diffusion length (typically 2-3 mm for n-type solar Si), so the CPC structure would be on the order of a few to several mm tall.

Similar to the previous section, we incorporate the ray tracing results into the detailed balance model. We also include the losses from the non-ideal reflector between the CPC apertures. Thus, the fraction of the light that escapes, P_{esc}, replacing $\sin^2(\theta_e)$, is now expressed as:

$$P_{esc} = \bar{T}(\lambda) + A_r(1 - R_t)n_g^2 \tag{7}$$

where $\bar{T}$ is the angle-averaged transmission determined from ray tracing, A_r is the fraction of the top surface area covered by the reflector, and R_t is the reflectivity of reflector which covers the top surface of the cell between the CPC output apertures, assumed to be 98% in this case. n_g is the refractive index of the material between the solar cell and reflector, which is assumed to be 1.5.

Using the above expression, we calculate the efficiency as a function of cell thickness for both the ideal and heterojunction cell models for two different CPC designs. The narrower CPC shape is defined by a 5°àcceptance angle with a 57°òutput angle, with an effective angle restriction of 10°. The broader CPC geometry has a 15°àcceptance angle with an 83°òutput angle, with an effective 25°àngle restriction. Refraction at the glass-air interface leads to the larger effective acceptance angle [29]. As shown in Figure 6c, for the smaller escape angles, the efficiency improvements suggested by Figures 1 and 2 are realizable. For the heterojunction structure, $0.8\%_{\text{abs}}$ efficiency improvement is found for the CPC structure with 10°èscape angle, with the optimal thickness decreasing substantially to 62 μm. For the CPC structure with a larger, 25°, escape angle an efficiency enhancement of $0.6\%_{\text{abs}}$ is observed. Such a structure would also allow for cheaper, less accurate tracking and more utilization of diffuse light. For the ideal cell, Figure 6c shows the effects of the CPC geometry are larger, with optimal thicknesses as thin as 10 μm and efficiency increases of $1.5\%_{\text{abs}}$. Thus, significant efficiency benefits for silicon solar cells are possible with realistic angle-restricting optical structures.

IV. Conclusions

Restricting the light escape angle with an external optic has significant potential to further improve the performance of silicon solar cells by improving light trapping, allowing for thinner, more efficient cells in a flat plate geometry. Using a detailed balance approach, we have re-evaluated the ideal, Auger-limited case and found that efficiency increases of up to $3\%_{\text{abs}}$ may be expected with very thin cells and narrow angle restriction. Considering the performance characteristics of record heterojunction and homojunction cells, we have found that the efficiency benefits of angle restriction are most significant in the heterojunction case, with $1.0\%_{\text{abs}}$ efficiency increases expected for cells that are half as thick as current optimum cells. Unlike the idealized case, for heterojunction and

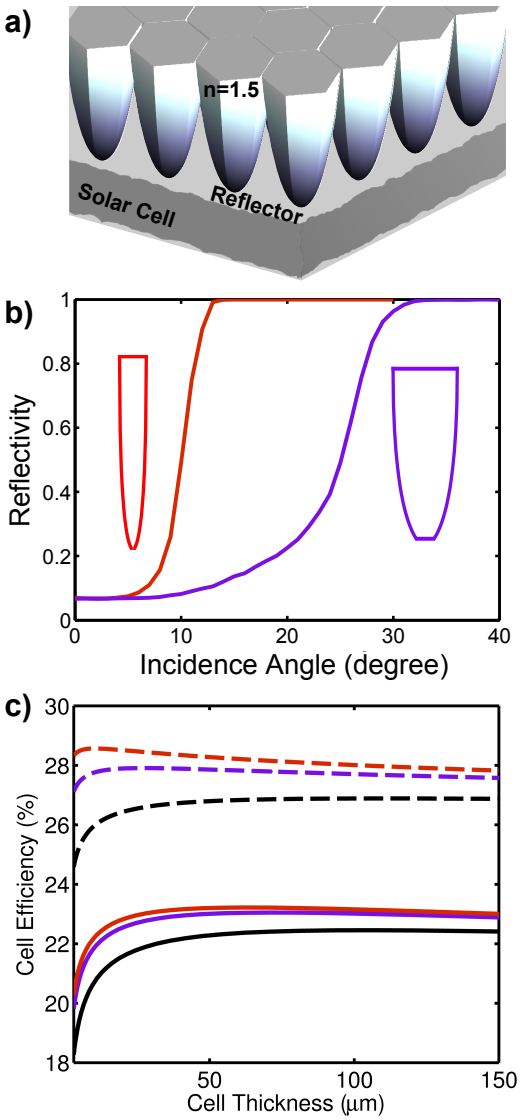

Fig. 6. a) CPC based ray-optical angle restrictor schematic. b) Reflectivity as a function of incident angle from ray-tracing simulations at 1000 nm wavelength for two CPC shapes (shown in insets) with effective angle restriction of 10°(red) and 25°(purple) respectively. c) The calculated efficiency as a function of thickness for the heterojunction cell model (solid lines) and ideal cell model (dashed lines) are shown for graded index AR coating (black) and the CPC arrays (red and purple according to (b)).

homojunction devices with surface and bulk recombination as well as parasitic optical losses, we find that limiting the escape angle more narrowly than 10°has minimal additional benefit. Low surface recombination velocity and excellent back reflectivity, as found in heterojunction cells, are crucial to achieving the maximal efficiency benefits with angle restriction. Angle restriction may also be used in concert with low to moderate external concentration, for addition efficiency enhancements. Finally, we have considered both narrowband rugate-based and broadband ray-optical angle restrictor designs. With the rugate structure, narrow escape angles are limited to a specific bandwidth (in this case 1050-1200 nm), and efficiency benefits are modest for both the heterojunction and ideal structures, with small changes in the optical thickness. In contrast, broadband angle restrictors can result in narrower escape angles, and show significant efficiency benefits and reductions in the optimal cell thickness. Based on these calculations, recent results with combined interdigitated back contact and heterojunction with intrinsic layer technology [1], and recently demonstrated technologies for micro-CPC based structures [7], [37] and high quality thin c-Si substrates [38]–[41] make this concept particularly relevant today. We envision broadband angle restriction with a CPC-based ray optical structure used in either a flat plate geometry or with low to moderate external concentration to enhance the performance of crystalline silicon solar cells as they approach fundamental materials limitations.

ACKNOWLEDGEMENTS

We thank M. Sheldon, H. Emmer and W. Sinke for insightful discussions and advice on the manuscript.

REFERENCES

[1] P. P. Release, "Panasonic HIT© solar cell: 25.6% efficiency world record," April 10, 2014, http://eu-solar.panasonic.net/en.
[2] E. Yablonovitch, "Statistical ray optics," *Journal of the Optical Society of America*, vol. 72, no. 7, 1982.
[3] P. Campbell and M. Green, "The limiting efficiency of silicon solar cells under concentrated sunlight," *IEEE Transacations on Electron Devices*, vol. ED-33, pp. 234–239, 1986.
[4] A. Martí, J. Balenzategui, and R. Reyna, "Photon recycling and Shockely's diode equation," *Journal of Applied Physics*, vol. 82, no. 8, pp. 4067–4075, 1997.
[5] A. Braun, E. Katz, D. Feuermann, B. Kayes, and J. M. Gordon, "Photovoltaic performance enhancement by external recycling of photon emission," *Energy and Environmental Science*, vol. 6, pp. 1499–1503, 2013.
[6] O. Höhn, T. Kraus, G. Bauhuis, U. T. Schwarz, and B. Bläsi, "Maximal power output by solar cells with angular confinement," *Optics Express*, vol. 22, no. S3, pp. A715–A722, May 2014.
[7] E. Kosten, J. Atwater, J. Parsons, A. Polman, and H. Atwater, "Highly efficient GaAs solar cells by limiting light emission angle," *Light: Science and Applications*, vol. 2, 2013.
[8] A. Richter, M. Hermle, and S. Glunz, "Reassessment of the limiting efficiency for crystalline silicon solar cells," *IEEE Journal of Photovoltaics*, vol. 3, no. 4, pp. 1184–1191, Oct 2013.
[9] A. Richter, S. Glunz, F. Werner, J. Schmidt, and A. Cuevas, "Improved quantitative description of auger recombination in crystalline silicon," *Physical Review B*, vol. 86, p. 165202, Oct 2012.
[10] A. Schenk, "Finite-temperature full random-phase approximation model of band gap narrowing for silicon device simulation," *Journal of Applied Physics*, vol. 84, no. 7, pp. 3684–3695, 1998.
[11] M. Taguchi, A. Yano, S. Tohoda, K. Matsuyama, Y. Nakamura, T. Nishiwaki, K. Fujita, and E. Maruyama, "24.7% record efficiency HIT solar cell on thin silicon wafer," *IEEE Journal of Photovoltaics*, vol. 4, no. 1, pp. 96–99, Jan 2014.
[12] P. Cousins, D. Smith, H.-C. Luan, J. Manning, T. Dennis, A. Waldhauer, K. Wilson, G. Harley, and W. Mulligan, "Generation 3: Improved performance at lower cost," in *Photovoltaic Specialists Conference (PVSC), 2010 35th IEEE*, June 2010, pp. 000 275–000 278.
[13] M. A. Green, K. Emery, Y. Hishikawa, W. Warta, and E. D. Dunlop, "Solar cell efficiency tables (version 42)," *Progress in Photovoltaics*, vol. 21, no. 5, pp. 827–837, 2013. [Online]. Available: http://dx.doi.org/10.1002/pip.2404
[14] A. Luque, "The confinement of light in solar cells," *Solar Energy Materials*, vol. 23, 1991.
[15] S. Fahr, C. Ulbrich, T. Kirchartz, U. Rau, C. Rockstuhl, and F. Lederer, "Rugate filter for light-trapping in solar cells," *Optics Express*, vol. 16, no. 13, pp. 9332–9343, 2008.
[16] C. Ulbrich, S. Fahr, J. Upping, M. Peters, T. Kirchartz, C. Rockstuhl, R. Wehrspohn, A. Gombert, F. Lederer, and U. Rau, "Directional selectivity and ultra-light-trapping in solar cells," *Physics Status Solidi A*, vol. 205, no. 12, pp. 2831–2843, 2008.

[17] P. Bermel, C. Luo, L. Zeng, L. C. Kimerling, and J. D. Joannopoulos, "Improving thin-film crystalline silicon solar cell efficiencies with photonic crystals," *Optics Express*, vol. 15, no. 25, pp. 16 986–17 000, Dec 2007. [Online]. Available: http://www.opticsexpress.org/abstract.cfm?URI=oe-15-25-16986

[18] W. Shockley and H. Queisser, "Detailed balance limit of efficiency of p-n junction solar cells," *Journal of Applied Physics*, vol. 32, no. 3, pp. 510–519, 1961.

[19] M. A. Green, "Self-consistent optical parameters of intrinsic silicon at 300k including temperature coefficients," *Solar Energy Materials and Solar Cells*, vol. 92, no. 11, pp. 1305 – 1310, 2008. [Online]. Available: http://www.sciencedirect.com/science/article/pii/S0927024808002158

[20] S. Sze and K. Ng, *Physics of Semiconductor Devices*. Wiley-Interscience, 1998.

[21] P. P. Altermatt, A. Schenk, F. Geelhaar, and G. Heiser, "Reassessment of the intrinsic carrier density in crystalline silicon in view of band-gap narrowing," *Journal of Applied Physics*, vol. 93, no. 3, pp. 1598–1604, 2003. [Online]. Available: http://scitation.aip.org/content/aip/journal/jap/93/3/10.1063/1.1529297

[22] A. Sproul and M. Green, "Intrinsic carrier concentration and minority carrier mobility of silicon from 77 to 300 k," *Journal of Applied Physics*, vol. 73, no. 3, pp. 1214–1225, Feb 1993.

[23] O. D. Miller, E. Yablonovitch, and S. R. Kurtz, "Strong internal and external luminescence as solar cells approach the Shockley-Queisser limit," *Photovoltaics, IEEE Journal of*, vol. 2, no. 3, pp. 303–311, July 2012.

[24] T. Tiedje, E. Yablonovitch, G. Cody, and B. Brooks, "Limiting efficiency of silicon solar cells," *IEEE Transactions on Electron Devices*, vol. ED-31, pp. 711–716, 1984.

[25] I. Schnitzer, E. Yablonovitch, C. Caneau, and T. Gmitter, "Ultrahigh spontaneous emission quantum efficiency, 99.7% internally and 72% eternally, from AlGaAs/GaAs/AlGaAs double heterostructures," *Applied Physics Letters*, vol. 62, no. 2, pp. 131–133, 1992.

[26] J. Nelson, *The Physics of Solar Cells*. Imperial College Press, 2003.

[27] ASTM Standard G173-03R12, *Standard Tables for Reference Solar Spectral Irradiances: Direct Normal and Hemispherical on 37° Tilted Surface.*, 14th ed. West Conshocken, PA: ASTM International, 2012, www.astm.org.

[28] Z. Holman, A. Descoeudres, L. Barraud, F. Fernandez, J. Seif, S. De Wolf, and C. Ballif, "Current losses at the front of silicon heterojunction solar cells," *IEEE Journal of Photovoltaics*, vol. 2, no. 1, pp. 7–15, Jan 2012.

[29] W. Welford and R. Winston, *High Collection Nonimaging Optics*. Academic Press, 1989.

[30] B. Saleh and M. Teich, *Fundamentals of Photonics, 2nd Ed.* Wiley, 2007.

[31] B. G. Bovard, "Rugate filter theory: an overview," *Applied Optics*, vol. 32, no. 28, pp. 5427–5442, 1993.

[32] W. H. Southwell, "Using apodization functions to reduce sidelobes in rugate filters," *Applied Optics*, vol. 28, no. 23, pp. 5091–5094, 1989.

[33] W. J. Gunning, R. L. Hall, F. J. Woodberry, W. H. Southwell, and N. S. Gluck, "Codeposition of continuous composition rugate filters," *Applied Optics*, vol. 28, no. 14, pp. 2945–2948, 1989.

[34] J.-S. Chen, S. Chao, J.-S. Kao, H. Niu, and C.-H. Chen, "Mixed films of TiO2—SiO2 deposited by double electron-beam coevaporation," *Applied Optics*, vol. 35, no. 1, pp. 90–96, 1996.

[35] H. Demiryont, "Optical properties of SiO2-TiO2 composite films," *Applied Optics*, vol. 24, no. 16, pp. 2647–2650, 1985.

[36] W. H. Southwell, "Gradient-index antireflection coatings," *Optics Letters*, vol. 8, no. 11, pp. 584–586, 1983.

[37] J. H. Atwater, P. Spinelli, E. Kosten, J. Parsons, C. Van Lare, J. Van de Groep, J. Garcia de Abajo, A. Polman, and H. A. Atwater, "Microphotonic parabolic light directors fabricated by two-photon lithography," *Applied Physics Letters*, vol. 99, no. 15, 2011.

[38] K. V. Nieuwenhuysen, M. R. Payo, I. Kuzma-Filipek, J. V. Hoeymissen, G. Beaucarne, and J. Poortmans, "Epitaxially grown emitters for thin film silicon solar cells result in 16% efficiency," *Thin Solid Films*, vol. 518, no. 6, Supplement 1, pp. S80 – S82, 2010, sixth International Conference on Silicon Epitaxy and Heterostructures. [Online]. Available: http://www.sciencedirect.com/science/article/pii/S0040609009017040

[39] P. Rosenits, F. Kopp, and S. Reber, "Epitaxially grown crystalline silicon thin-film solar cells reaching 16.5% efficiency with basic cell process," *Thin Solid Films*, vol. 519, no. 10, pp. 3288 – 3290, 2011. [Online]. Available: http://www.sciencedirect.com/science/article/pii/S0040609010017992

[40] R. A. Rao, L. Mathew, S. Saha, S. Smith, D. Sarkar, R. Garcia, R. Stout, A. Gurmu, E. Onyegam, D. Ahn, D. Xu, D. Jawarani, J. Fossum, and S. Banerjee, "A novel low cost 25μm thin exfoliated monocrystalline Si solar cell technology," in *Photovoltaic Specialists Conference (PVSC), 2011 37th IEEE*, June 2011, pp. 001 504–001 507.

[41] J. H. Petermann, D. Zielke, J. Schmidt, F. Haase, E. G. Rojas, and R. Brendel, "19%-efficient and 43 μm-thick crystalline Si solar cell from layer transfer using porous silicon," *Progress in Photovoltaics: Research and Applications*, vol. 20, no. 1, pp. 1–5, 2012. [Online]. Available: http://dx.doi.org/10.1002/pip.1129

Emily D. Kosten Emily D. Kosten recently defended her Ph.D. in physics at the California Institute of Technology, Pasadena, CA where she was the recipient of a Resnick Sustainability Institute Graduate Fellowship. Her Ph.D. research in the Atwater group focused on optical design and the thermodynamic limits of solar cell efficiency. After completing her studies at Caltech, she will join the technical staff of MIT Lincoln Laboratory.

Bonna K. Newman Bonna Newman received her Ph.D. in physics at the Massachusetts Institute of Technology, Cambridge, MA in 2008. She was a Clare Boothe Luce Postdoctoral Fellow in the Laboratory for Photovoltaics at MIT researching defect engineering in materials for photovoltaics from 2008 until 2010. From 2011-2013, she was a Senior Member of the Technical Staff at Twin Creeks Technologies in San Jose, CA, developing HIT cells on c-Si substrates less than 20 μm thick. She joined the Center for Nanophotonics, FOM Institute AMOLF, Amsterdam, Netherlands in 2013 to study the application of nanophotonic concepts to solar cell devices and recently joined the research staff at ECN Solar Energy, Petten, Netherlands. Her research interests include light capture on thin Si substrates, nanostructured PV, and advanced device concepts with industrial viability.

John V. Lloyd John Lloyd is a Ph.D. candidate at the California Institute of Technology in Pasadena, CA. He received a B.S. and an M.S in materials science and engineering from Drexel University in Philadelphia, PA, in 2010. His current research interests include optical strategies for enhancing photovoltaic energy conversion efficiencies.

Albert Polman Biography text here.

Harry A. Atwater Harry Atwater is the Howard Hughes Professor of Applied Physics and Materials Science at the California Institute of Technology. Professor Atwater currently serves as Director of the DOE Energy Frontier Research Center on Light-Material Interactions in Solar Energy Conversion, and is also Director of the Resnick Sustainability Institute, Caltechs largest endowed research program. Atwaters scientific interests have two themes: photovoltaics and solar energy as well as plasmonics and optical metamaterials. His group has created new high efficiency solar cell designs, and have developed principles for light trapping. Atwater is an early pioneer in nanophotonics and plasmonics; he gave the name to the field of plasmonics in 2001. He has authored or co-authored more than 400 publications cited in aggregate ¿ 20,000 times and his groups advances in the solar energy and plasmonics field have been reported in Scientific American, Science, Nature Materials, Nature Photonics and Advanced Materials. He is the founding Editor-in-Chief of ACS Photonics and serves as Associate Editor for the IEEE Journal of Photovoltaics. In 2006 he founded the Gordon Research Conference on Plasmonics, which he served as chair in 2008. He is co-founder and chief technical advisor for Alta Devices, a venture-backed company in Santa Clara, CA, currently developing high efficiency/low cost GaAs photovoltaics technology, and of Caelux Corporation, a venture-backed photovoltaics company in Pasadena, CA.